A Billet Heat Transfer Modeling during Reheating Furnace Operation

Yu Jin Jang* and Sang Woo Kim**

*Electrical and Computer Engineering Division, POSTECH, Pohang, 790-784, Korea
(Tel: +82-54-279-5018; Fax: +82-54-279-2903; Email: season@postech.ac.kr)
**Electrical and Computer Engineering Division, POSTECH, Pohang, 790-784, Korea
(Tel: +82-54-279-2237; Fax: +82-54-279-2903; Email: swkim@postech.ac.kr)

Abstract: Reheating furnace is an essential facility of a rod mill plant where a billet is heated to the required rolling temperature so that it can be milled to produce wire. Sometimes, it is also necessary to control a transient billet temperature pattern according to the material characteristics to prevent a wire from breaking. Though it is very important objective to obtain a correct information of billet temperatures, it is not feasible to obtain an on-line information of a billet temperature during furnace operation. Consequently, a billet temperature profile must be estimated. In this paper, a billet heat transfer model based on FEM (Finite Element Method) with spatially distributed emission factors is proposed and a measurement is also carried out for two different furnace operation conditions. Finally, the difference between the model outputs and the measurements is minimized by using the new optimization algorithm named uDEAS (Univariate Dynamic Encoding Algorithm for Searches) with multi-step tuning strategy. Hence, the information of billet temperatures can be obtained by using proposed model on various furnace operation conditions.

Keywords: Reheating furnace, Billet temperature estimation, Emission factors, FEM, uDEAS

1. Introduction

Wire is produced by sending a billet to a rolling machine at rod mil plant. In this process, the billet is heated in a reheating furnace and it should be heated as closely as possible to the required rolling temperature to be milled without any damage to the roller. Typical reheating furnace has three zones (i.e, preheating, heating, and soaking zones) [1]-[5],[11] and some new reheating furnaces have one more soaking zone. After a billet is charged into a reheating furnace, the billet goes through these zones from inlet to outlet and finally it reaches a target temperature. Though it is a fundamental objective of the reheating furnace to heat up the billet to the target temperature, sometimes, in addition to that objective, it is also necessary to control a transient billet temperature pattern according to the material characteristics to prevent a wire from breaking. For example, a steel cord, which is used as a tire reinforcement material, is made of very thin high-carbon steel wire. In general, a billet with a high carbon content has carbon segregation at center side owing to the difference of cooling speed between the billet surface and center after casting. This carbon segregation is one of the major cause of wire-breaking in wire production process. Fortunately, the effect of the carbon segregation can be minimized by controlling the billet temperature according to the predefined special billet temperature pattern in the furnace. Therefore, it is very important to obtain a correct information of billet temperatures. However, it is not feasible to obtain an on-line information of a billet temperature during reheating furnace operation. Consequently, a billet temperature profile must be estimated.

This paper proposes a billet heat transfer model based on FEM and an optimization algorithm named uDEAS to estimate the billet temperature during the reheating furnace operation. Temperatures of the billet and ambient furnace gas are measured for two different furnace operating patterns. A 2D FEM heat transfer model of the billet with nonlinear specific heat and thermal conductivity is constructed. In this 2D FEM model, though only a radiative heat transfer term with an emission factor is considered at the boundary of the billet, the effect of convective heat transfer between billet and its ambient gas and conductive heat transfer between billet and skid button are taken into account by controlling the emission factor. In this paper, it is assumed that emission factor is a function of position. By this assumption, the furnace is divided into 10 parts along the billet moving path and different emission factors are applied on top, bottom and left/right sides of the billet at each part. Subsequently, the difference between the measured billet temperatures and the estimated billet temperatures obtained from the FEM model is minimized by tuning the above 30 emission factors according to the following tuning strategy: 1. Set the emission factors of the billet left/right sides as that of billet top side and then tune these emission factors. 2. Fix the emission factors of the billet top and bottom sides and then tune the emission factors of the billet left/right sides. 3. Fix the emission factors of the billet left/right sides and then tune the emission factors of the billet top and bottom sides. 4. Repeat step 2 once. At this tuning process, uDEAS, which is an effective and easily applicable optimization algorithm, is applied with different cost functions to obtain those optimal emission factors. Hence, the information of billet temperatures can be obtained by using proposed model on various furnace operation conditions.

2. Reheating furnace and billet temperature measurement [4]

The reheating furnace at rod mill plant of POSCO (Pohang Iron & Steel Co., Ltd.) consists of four zones (i.e., preheating, heating and soaking zone 1 and 2) and it has two tracks (i.e., billet-moving paths) as shown in Fig. 1(a). The billets

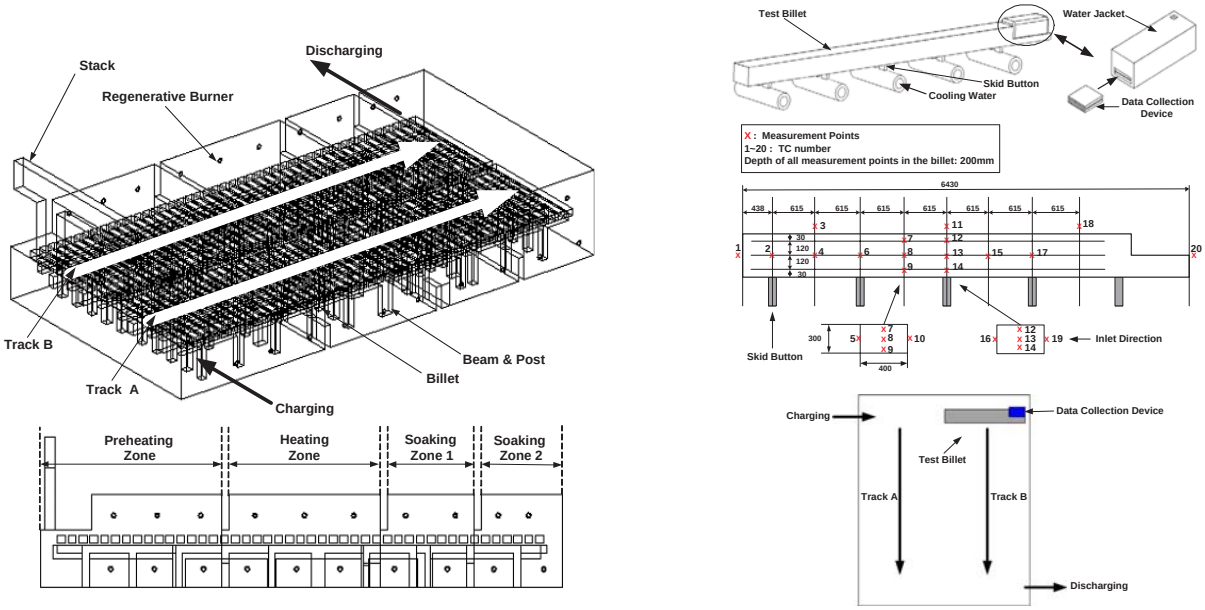

(a) Furnace structure (b) Experiment setting

Fig. 1. Furnace structure and billet temperature measurement

move along the track slowly. Also 16, 14, 9 and 6 billets are contained in preheating, heating, soaking zone 1 and 2, respectively, on each track. Therefore, there are 90 billets in the furnace. This furnace is divided into four zones more clearly than the conventional furnace. Also, the exhaust gas is discharged through opposite burner by 80% owing to the operating mechanism of the regenerative burner. Hence, the interference of neighboring zones is reduced significantly compared with the conventional furnace.

Billet temperatures are measured by using a data collection device mounted on a billet as shown in Fig. 1(b). In many literatures, total measurement points of billet temperature and ambient gas temperature are just $3 \sim 5$ points. Since these number of measurement points are insufficient for observation of billet temperature distribution, 20 points are selected for measurement by using TC (thermocouples). The data collection device is put into a water jacket which is filled with water. This water jacket is covered with heat protective material to minimize exposure to heat radiation. When the test billet is discharged from the furnace, the data collection device is removed and the stored data are transferred to a PC using a serial cable. This measurement is carried out for the following two typical furnace operation patterns:

1. CCR (Cold Charge Rolling) pattern: An operation pattern when the billet with a normal temperature is charged.
2. WCR (Warm Charge Rolling) pattern: An operation pattern when the billet with high initial temperature is charged.

It is observed that the measured temperatures have several characteristics as follows:

1. The ambient temperature of the billet top side along the track is not uniform at the same zone (TC_{11}).
2. The ambient temperature of the billet at a furnace center side is higher than the ambient temperature at furnace wall sides.($TC_{1,3,11,18,\ and\ 20}$).
3. The ambient temperature of the billet right side (TC_{16}) is higher than the temperature of the billet left side (TC_{19}). The temperature difference between them decreases as the billet is transported through the furnace. Finally, $TC_{11,16,\ and\ 19}$ have similar values at the soaking zones.
4. At the same zone, $(TC_{11} - TC_{16})$ and $(TC_{11} - TC_{19})$ have maximum and minimum value at the beginning and end of each zone, respectively.
5. Also, the billet core temperature (i.e., $TC_{2,4,6,8,13,15,\ and\ 17}$) at the furnace center side is higher than the core temperature at the furnace wall side. For example, $(TC_2 - TC_{17})$ is about $60^{\circ}C$ when the billet is discharged.

Since the part of the billet which is on the skid button is called skid part, measurement points within the billet can be classified into skid and non-skid parts. The temperatures of the skid and non-skid parts are measured using TC installed in holes that go into 10%, 50%, and 90% along the billet thickness direction as shown in Fig. 1(b) (i.e., $TC_{7,8,\ and\ 9}$ for non-skid part and $TC_{12,13,\ and\ 14}$ for skid part). Only the temperature profiles of skid part will be used for billet heat transfer modeling in the next section.

3. Heat transfer model

In this section, a non-linear specific heat and thermal conductivity of the test billet are given and then a billet heat transfer model using 2D FEM with spatially distributed emission factors is introduced.

3.1. Material properties [4]

The billet, which is used in the above measurement, consists of the following chief ingredients: (C[%] : $0.326 \sim 0.384$, Si[%] : $0.15 \sim 0.30$, Mn[%] : $0.70 \sim 0.80$, P[%] : $max.\ 0.20$, S[%] : $max.\ 0.15$). Since it is well known that a specific heat and thermal conductivity of the billet are mainly depends on a carbon content, these approximate material properties

of the test billet are obtained by using 0.4% carbon content, which is a similar carbon content of the test billet, as shown in Fig. 2 [6].

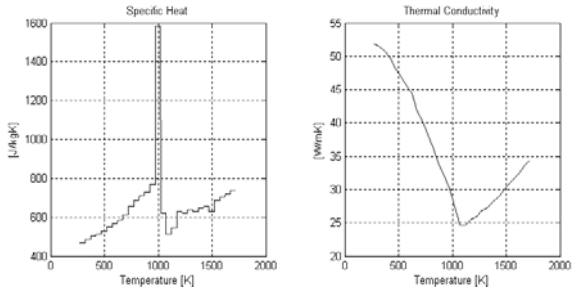

Fig. 2. Material Properties

3.2. FEM model

The heat transfer between the billet and the furnace is considerably complex. It consists of the following factors [7]: 1. Radiation from furnace walls, 2. Radiation from gas, 3. Convection from gas, 4. Heat conduction to skid buttons, 5. Heat transfer between the billets. Though a 1D PDE (Partial Differential Equation) model with FEM is adopted to describe the heat transfer of the slab [7],[8], a 2D PDE model with FEM is suitable for our problem owing to the shape of the billet as shown in Fig. 1(b). In this paper, only skid part is used for modeling.

Nomenclature

T : *billet temperature* $[K]$
t : *time* $[sec]$
ρ : *density of the billet* $= 7800\ [kg/m^3]$
c : *specific heat* $[J/kgK]$
k : *thermal conductivity* $[W/mK]$
x, y : *coordinate of 2D domain* $[m]$

The heat transfer in the billet is represented as follows [9]-[11]:

$$\rho c(T)\frac{\partial T}{\partial t} = \frac{\partial}{\partial x}\left(k(T)\frac{\partial T}{\partial x}\right) + \frac{\partial}{\partial y}\left(k(T)\frac{\partial T}{\partial y}\right). \quad (1)$$

The weighted residual form of (1) is

$$\int_\Omega W\left[\frac{\partial T}{\partial t} - \frac{\partial}{\partial x}\left(\alpha\frac{\partial T}{\partial x}\right) - \frac{\partial}{\partial y}\left(\alpha\frac{\partial T}{\partial y}\right)\right]d\Omega = 0 \quad (2)$$

where $\alpha = k(T)/\rho c(T)$ and Ω denotes the two-dimensional domain. After applying Green's theorem, (2) can be represented as follows [10]:

$$\int_\Omega \left[W\frac{\partial T}{\partial t} + \alpha\left(\frac{\partial W}{\partial x}\frac{\partial T}{\partial x} + \frac{\partial W}{\partial y}\frac{\partial T}{\partial y}\right)\right]d\Omega + \int_{\Gamma_B} W\left(-\alpha\frac{\partial T}{\partial n}\right)d\Gamma = 0 \quad (3)$$

where Γ_B denotes the boundary and $d\Gamma$ denotes the surface element of Γ_B over which the normal gradients are applied.

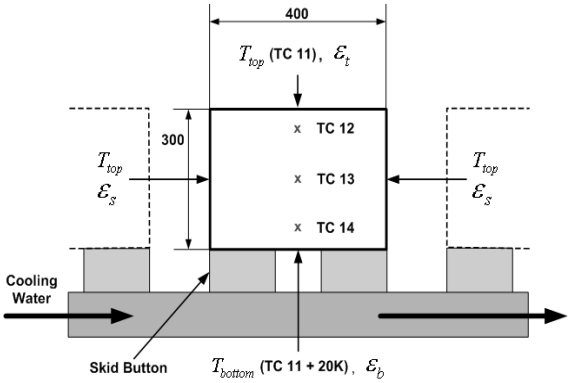

(a) Boundary conditions

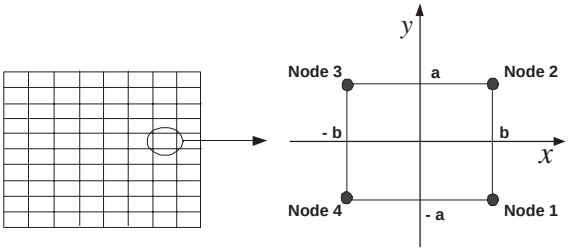

(b) 8x10 mesh generation by using bilinear rectangular element

Fig. 3. Boundary conditions and mesh generation

Also n denotes the outward normal unit vector at the boundary Γ. Since the bilinear rectangular element is used as a shape function as shown in Fig. 3(b), T and α are approximated using this shape function as follows:

$$\begin{aligned} T(x,y,t) &= \Sigma_{i=1}^4 H_i(x,y)T_i(t) \\ \alpha(x,y) &= \Sigma_{i=1}^4 H_i(x,y)\alpha_i \end{aligned} \quad (4)$$

where H_i and α_i are the value of H and α at the node i, respectively, and

$$H_1 = \frac{(b-x)(a-y)}{4ab}, \quad H_2 = \frac{(b+x)(a-y)}{4ab}$$
$$H_3 = \frac{(b+x)(a+y)}{4ab}, \quad H_4 = \frac{(b-x)(a+y)}{4ab}.$$

The discrete model is obtained by the Galerkin's method with substituting (4) into (3) and setting $W_i = H_i$. A detailed description is given in [9],[10].

In this FEM model, 80 bilinear rectangular elements are used and ambient temperatures of the billet are set as shown in Fig. 3(a). The ambient temperature of the billet left and right sides (i.e., a space between billets) is assumed as T_{top}. This can be easily guessed by the observation of the experimental results 3 and 4 in the previous section. The furnace temperatures are measured by using sensors attached on top and bottom of the furnace. Since the furnace temperature of the bottom is set higher by $20K$ than that of the top, the assumption of the ambient temperature of the billet bottom side, $T_{bottom} = T_{top} + 20K$, is appropriate.

Radiative heat transfer at the boundary is represented as follows:

$$-k\frac{\partial T}{\partial n} = 5.67 \times 10^{-8}(T^4 - T_{amb}^4) \times \epsilon \quad (5)$$

where ϵ is an emission factor. Since the emission factor is different according to the geometry between billet surface and furnace, different emission factors, ϵ_t, ϵ_b, and ϵ_s are applied on top, bottom and left/right sides of the billet as shown in Fig. 3(a).

3.3. Controlling billet heat transfer with spatially distributed emission factors

Though only radiative heat transfer is considered as a boundary condition, convective and conductive heat transfer at skid part are also considered by controlling the above emission factors (i.e., ϵ_t, ϵ_b, and ϵ_s). However, it is not satisfactory to use constant emission factors because these emission factors vary according to the geometry between the billet and furnace. Hence, for simplicity, it is assumed that the emission factor is a function of position along the track. By this assumption, the furnace is divided into 10 parts, $P_1 \sim P_{10}$, along the track as shown in Fig. 4 and different emission factors are applied on top, bottom and left/right sides of the billet at each part (i.e., $\epsilon_{t1} \sim \epsilon_{t10}$ for the billet top side, $\epsilon_{b1} \sim \epsilon_{b10}$ for the billet bottom side, and $\epsilon_{s1} \sim \epsilon_{s10}$ for the billet left/right side). $T_{ave(CCR)}$ and $T_{ave(WCR)}$ represent average ambient temperature values measured at the top and bottom sides of the furnace for the CCR and WCR patterns, respectively. They have similar patterns except the preheating zone. If the above emission factors are given, the profiles of the billet temperature can be obtained by using the Crank-Nicolson method [9],[10] with the above FEM model and boundary conditions.

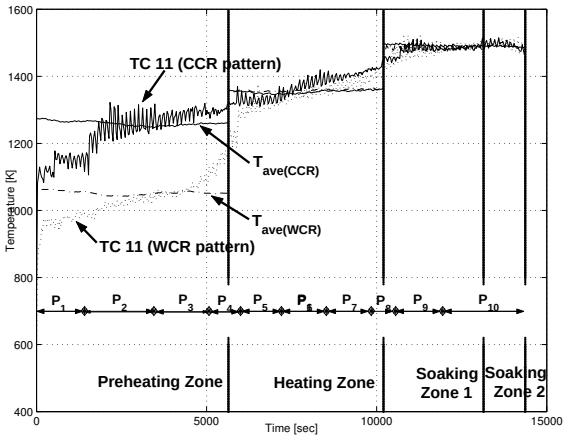

Fig. 4. Division of furnace along the track

4. Adapting the model to the measurement using uDEAS

Searching for optimal emission factors, which minimize error between measurements and model outputs, with conventional optimization algorithms is not an easy task. In this paper, a new optimization algorithm named uDEAS, which is effective and easily applicable, is employed to tune the 30 emission factors. At this step, the emission factors are tuned by using a multi-step tuning strategy.

4.1. uDEAS [4]

Dynamic Encoding Algorithm for Searches (DEAS) has been developed as a new type of non-gradient optimization method since 2002 [12],[13]. The principle of DEAS is based on the distinct properties of binary strings. If a binary digit, 0 or 1, is appended to any binary string as a least significant bit (LSB), the decoded real number of a new binary string decreases for 0, and increases for 1 compared with that of the original binary string (i.e., bisectional search, BSS). Moreover, if a binary string undergoes increment addition or decrement subtraction, the real number of each processed string increases or decreases equidistantly (i.e., unidirectional search, UDS). These two characteristics of binary strings are adopted for the determination of search directions and step lengths in a local search phase. For a global search strategy, the multistart approach is embedded into DEAS with various revisit check functions for search efficiency. Details are found in a dedicated website 'www.deasgroup.net'. DEAS is now classified into two categories; exhaustive DEAS (eDEAS) and univariate DEAS (uDEAS). eDEAS is an original version of DEAS with the above-mentioned local search principles which suffer from exponential complexity as search dimension increases. uDEAS is especially designed for lightening the exponential computation burden in local search by modifying the philosophy of 'BSS for every parameter-UDS for every parameter' into the philosophy of 'BSS-UDS for each parameter in a sequential manner'. Owing to its simple structure, uDEAS requires no redundancy check routine [13] and its amount of cost evaluation for a single optimal transition is decreased from $O(2^n)$ to $O(2n)$. This difference results in enormous computational reduction in real world large-scaled systems. Effectiveness of uDEAS has been validated with the well-known benchmark functions whose landscapes are nonsmooth and/or highly multimodal. uDEAS is also being applied to an on-load parameter identification of induction motors for diagnosis with successful results.

4.2. Adaptation strategy

The emission factors are found by simulating the FEM model and comparing the simulation results with the measured billet temperatures for skid part. Using uDEAS, the emission factors are found by minimizing SSE (Sum Squared Error) between the model outputs and measurements. Let TC_i^{est} be a model output which is corresponding to measured data of TC_i. The cost function with weighting factors, ρ_1, ρ_2 and ρ_3 is defined as follows:

$$\begin{aligned} &Cost\ Function\ = \\ &\sum_{CCR\ \ pattern} \rho_1 e_{top}^2 + \rho_2 e_{center}^2 + \rho_3 e_{bottom}^2 \\ &+ \sum_{WCR\ \ pattern} \rho_1 e_{top}^2 + \rho_2 e_{center}^2 + \rho_3 e_{bottom}^2 \end{aligned} \tag{6}$$

where $e_{top} = (TC_{12}^{est} - TC_{12})$, $e_{center} = (TC_{13}^{est} - TC_{13})$, and $e_{bottom} = (TC_{14}^{est} - TC_{14})$. Define *Cost Function 1* and *Cost Function 2* by choosing $(\rho_1, \rho_2, \rho_3) = (100, 1, 100)$ and $(\rho_1, \rho_2, \rho_3) = (1, 100, 1)$, respectively. Since the temperatures of the skid parts are measured only along the billet thickness direction, it is natural to divide the tuning process into two stage: 1. Tune the $\epsilon_{t1} \sim \epsilon_{t10}$ and $\epsilon_{b1} \sim \epsilon_{b10}$ while the $\epsilon_{s1} \sim \epsilon_{s10}$ are fixed. 2. Tune the $\epsilon_{s1} \sim \epsilon_{s10}$ while the $\epsilon_{t1} \sim \epsilon_{t10}$ and $\epsilon_{b1} \sim \epsilon_{b10}$ are fixed. At stage 1, since

the measured data, TC_{12} and TC_{14}, are available along the billet thickness direction, *Cost Function 1* is chosen to give priority to e_{top} and e_{bottom}. At stage 2, *Cost Function 2* is chosen to give priority to e_{center} because the measured data like TC_{12} and TC_{14} are not available along the billet width direction. This tuning process is carried out iteratively to give appropriate results. The tuning strategy is as follows:

step 1. Set the emission factors of the billet left/right sides as those of billet top side and then tune these emission factors with *Cost Function 1.*

step 2. Fix the emission factors of the billet top and bottom sides and then tune the emission factors of the billet left/right sides with *Cost Function 2.*

step 3. Fix the emission factors of the billet left/right sides and then tune the emission factors of the billet top and bottom sides with *Cost Function 1.*

step 4. Repeat step 2 once.

4.3. Results

The emission factors, which are restricted from 0 to 1, are obtained by using the above scheme for skid part as follows:

$$E \equiv \begin{bmatrix} \epsilon_{t1} & \dots & \epsilon_{t5} \\ \epsilon_{t6} & \dots & \epsilon_{t10} \\ \epsilon_{b1} & \dots & \epsilon_{b5} \\ \epsilon_{b6} & \dots & \epsilon_{b10} \\ \epsilon_{s1} & \dots & \epsilon_{s5} \\ \epsilon_{s6} & \dots & \epsilon_{s10} \end{bmatrix},$$

$$E = \begin{bmatrix} 0.7143 & 0.7302 & 0.6032 & 0.6825 & 0.8254 \\ 0.3492 & 0.5714 & 0.4762 & 0.5556 & 0.5079 \\ 0.9048 & 0.6667 & 0.7619 & 0.6825 & 0.7460 \\ 0.3492 & 0.4444 & 0.4127 & 0.1270 & 0.1111 \\ 0.5397 & 0.7619 & 0.2698 & 0.0000 & 0.6349 \\ 0.0159 & 1.0000 & 1.0000 & 1.0000 & 1.0000 \end{bmatrix} \quad (7)$$

The tuning results and its errors are shown in Fig. 5. Let T_s and T_m represent the simulated and measured billet center temperature, respectively. The billet center temperature and its error $(T_s - T_m)$ at discharging are shown in Table. 1. The maximum absolute error, $max\ |e_{center}|$, between the simulated and measured billet center temperatures is also shown in Table 2. Though the billet center temperatures at discharging after step 1 and 4 are similar, the corresponding maximum absolute errors during furnace operation are significantly reduced after step 4.

Table 1. Billet center temperature at discharging

	CCR pattern [K]			WCR pattern [K]		
TC 13	T_s	T_m	error	T_s	T_m	error
After step 1	1454.1	1447.8	6.3	1424.3	1421.1	3.2
After step 4	1454.8	1447.8	7	1425.7	1421.1	4.6

Table 2. Maximum absolute error of billet center temperature

$max\ \lvert e_{center}\rvert$ (CCR pattern)		$max\ \lvert e_{center}\rvert$ (WCR pattern)	
After step 1	After step 4	After step 1	After step 4
86 [K]	58.7 [K]	84.4 [K]	42 [K]

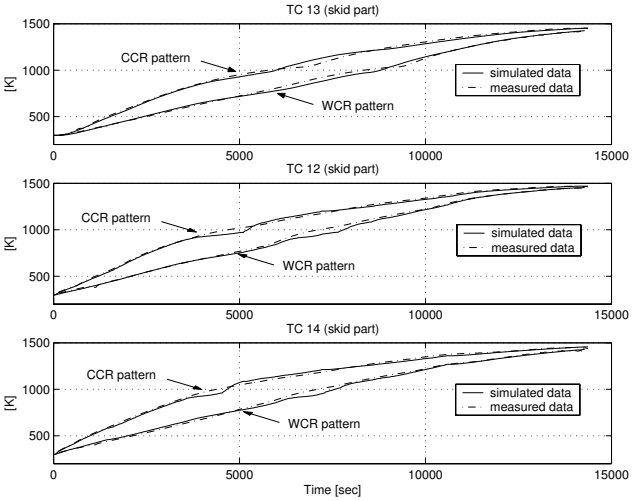

(a) Tuning results for the CCR/WCR pattern

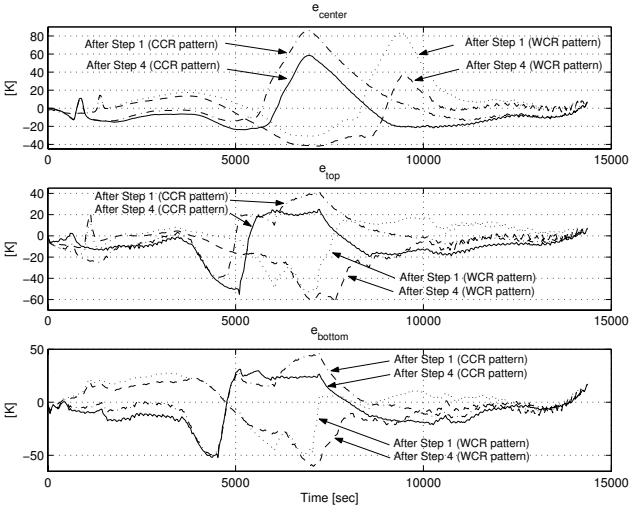

(b) Errors

Fig. 5. Tuning results and its errors

5. Concluding Remarks

In this paper, a 2D billet heat transfer FEM model with 30 emission factors is proposed to obtain an on-line information of billet temperatures during reheating furnace operation. At this step, the emission factors are assumed as a function of position and then these emission factors are obtained by applying the proposed tuning strategy, which consists of 4 steps, with the aid of uDEAS. The performance of the proposed model is shown by comparing the measured data with the corresponding model output.

References

[1] *Technical Report of Combustion Control for a Reheating Furnace 2nd ed.*, POSCON, 1999.

[2] Hyun Suk Ko, Jung-Su Kim, Tae-Woong Yoon, Mokeun Lim, Dae Ryuk Yang and Ik Soo Jun, *Modeling and Predictive Control of a Reheating Furnace*, Proc. American Control Conf., Chicago, Illinois, pp. 2725-2729, 2000.

[3] J. H. Choi, Y. J. Jang and S. W. Kim, *Temperature Control of a Reheating Furnace using Feedback Lin-*

earization and Predictive Control, International Conference on Control, Automation and Systems, Jeju, pp. 103-106, 2001.

[4] Yu Jin Jang, Jong-Wook Kim and Sang Woo Kim, *Design of Optimal Temperature Patterns in the Reheating Furnace with Regenerative Burner for Energy Saving*, unpublished.

[5] J. G. Kim and K. Y. Huh, *Prediction of Transient Slab Temperature Distribution in the Re-heating Furnace of a Walking-beam Type for Rolling of Steel Slabs*, ISIJ International, Vol. 40, No. 11, pp. 1115-1123, 2000.

[6] *A measurement of heat transfer in a reheating furnace and its computation method*, a subcommittee on reheating furnace, The Iron and Steel Institute of Japan, 1971.

[7] Pedersen, L. M., *Modeling and Control of Plate Mill Processes*, PhD thesis, Department of Automatic Control, Lund Institute of Technology, 1999.

[8] *FEMLAB Automatic Control Reference Manual*, COMSOL, 2000.

[9] Young W. Kwon and Hyochoong Bang, *The Finite Element Method Using MATLAB 2nd ed.*, CRC Press, 2000.

[10] Darrel W. Pepper and Juan C. Heinrich, *The Finite Element Method, Basic Concepts and Applications*, Hemisphere Pub. Corp., 1992.

[11] Yong-yao Yang and Yong-zai Lu, *Development of a Computer Control Model for Slab Reheating Furnaces*, Computers in Industry, 7, pp. 145-154, 1986.

[12] J. -W. Kim, S. J. Kim, and S. W. Kim, *Parameter identification of induction motors using dynamic encoding algorithm for searches (DEAS)*, IECON, pp. 150-155, Roanoke, VA, 2003.

[13] J. -W. Kim and S. W. Kim, *Parameter identification of induction motors using dynamic encoding algorithm for searches (DEAS)*, IEEE Trans. Energy Conversion, in press.